



**HAL**  
open science

# Magma degassing during the April 2007 collapse of Piton de la Fournaise: The record of semi-volatile trace elements (Li, B, Cu, In, Sn, Cd, Re, Tl, Bi)

Ivan Vlastélic, Gabrielle Menard, Abdelmouhcine Gannoun, Jean-Luc Piro, Thomas Staudacher, Vincent Famin

## ► To cite this version:

Ivan Vlastélic, Gabrielle Menard, Abdelmouhcine Gannoun, Jean-Luc Piro, Thomas Staudacher, et al.. Magma degassing during the April 2007 collapse of Piton de la Fournaise: The record of semi-volatile trace elements (Li, B, Cu, In, Sn, Cd, Re, Tl, Bi). *Journal of Volcanology and Geothermal Research*, 2013, 254, pp.94-107. 10.1016/j.jvolgeores.2012.12.027 . hal-00981449

**HAL Id: hal-00981449**

**<https://hal.science/hal-00981449>**

Submitted on 22 Nov 2021

**HAL** is a multi-disciplinary open access archive for the deposit and dissemination of scientific research documents, whether they are published or not. The documents may come from teaching and research institutions in France or abroad, or from public or private research centers.

L'archive ouverte pluridisciplinaire **HAL**, est destinée au dépôt et à la diffusion de documents scientifiques de niveau recherche, publiés ou non, émanant des établissements d'enseignement et de recherche français ou étrangers, des laboratoires publics ou privés.



Distributed under a Creative Commons Attribution - NonCommercial 4.0 International License

# Magma degassing during the April 2007 collapse of Piton de la Fournaise: The record of semi-volatile trace elements (Li, B, Cu, In, Sn, Cd, Re, Tl, Bi)

I. Vlastélic <sup>a,\*</sup>, G. Menard <sup>a</sup>, A. Gannoun <sup>a</sup>, J.-L. Piro <sup>a</sup>, T. Staudacher <sup>b</sup>, V. Famin <sup>c</sup>

<sup>a</sup> *Laboratoire Magmas et Volcans, Clermont Université, Université Blaise Pascal, CNRS UMR 6524, IRD R 163, France*

<sup>b</sup> *Observatoire Volcanologique du Piton de la Fournaise, Institut de Physique du Globe de Paris, Sorbonne Paris Cité, CNRS UMR 7154, France*

<sup>c</sup> *Laboratoire Géosciences Réunion, Université de la Réunion, Institut de Physique du Globe de Paris, Sorbonne Paris Cité, CNRS UMR 7154, France*

This study reports the concentrations of trace elements, including fluid mobile and semi-volatile species (e.g., Li, B, Cu, Re, In, Sn, Cd, Tl, Bi) in lavas erupted before and during the April 2007 collapse of the Piton de la Fournaise summit. Lavas erupted just prior to the collapse (April 5) display anomalous abundances in semi-volatile elements, with both depletion in Li, Cu and Tl (mostly on April 2) and enrichment in Cd, Bi, In and Sn (on April 3 and 4). These transient anomalies are thought to record unusual degassing conditions. Between March 30 and April 2, static decompression caused by magma withdrawal from the shallow magma reservoir might have triggered massive exsolution of a H<sub>2</sub>O- and S-rich phase in which Li and Cu might have partitioned. Alternatively, the Li–Cu depletion could record the degassing of a magma body that intruded at shallow depth during the same period. The Bi–Cd–In–Sn enrichment observed in the April 3–4 magmas requires conditions that prevent magma outgassing. In the absence of evidence for the pressurisation of the reservoir or the onset of collapse before April 5, it is suggested that the occurrence of less degassed lavas on April 3 and 4 reflects a high rate of magma transfer from the shallow magma reservoir to the eruption site just prior to summit collapse. The kinetic (diffusive) fractionation of elements accounts for the observed anomalies. The short time-scales required to fractionate Li from Cd diffusively (minutes to hours) and Cd from Bi (few hours to two days) support the idea that the magmas underwent rapid pressure variations a few days before the summit collapse.

## 1. Introduction

Réunion Island (60×40×3 km) is located in the Indian Ocean at 21°10'S, 55°30'E (Fig. 1a). It is the emergent part of a basaltic cone of 240×200×7 km. The island is the present location of the hotspot that created the Deccan Traps, the Chagos–Maldivé–Laccadive ridge, the Mascarene Plateau and Mauritius Island. The island is presently composed of two main volcanoes, the extinct Piton des Neiges in the NW and the active Piton de la Fournaise in the SE (Fig. 1b). Piton de la Fournaise has been regularly active since at least 530 ka (Gillot and Nativel, 1989) and is still presently in its shield building stage. Three major events, either collapses or landslides, marked the growth history of the volcano 250, 35 and 4.7 ka ago (Gillot et al., 1994). The result is three concentric calderas or depressions, the most recent of which (the Enclos Fouqué) is U-shaped (8×13 km) and open to the sea on its eastern side (Fig. 1c). A 400 m high cone with two coalescent summit craters (Bory and Dolomieu) rises inside the Enclos Fouqué.

Although collapse calderas are relatively common features of basaltic volcanoes, very few have been observed during their formation. The

collapse of the Piton de la Fournaise summit in April 2007 is one of these formations. Due to the advanced monitoring network, the timing of the events and the temporal relationship between the magma withdrawal from the shallow reservoir and the collapse of the summit crater in particular are known in detail (Michon et al., 2007; Staudacher et al., 2009). Since 1977, the emitted lavas have been sampled regularly during the course of the eruption, providing a unique opportunity to track compositional changes that may be linked to caldera-forming processes. Previous geochemical studies of the April 2007 samples (Villemant et al., 2009; Vlastélic et al., 2009; Collins et al., 2012) have discussed general issues related to the magma source, magma differentiation and degassing trends, but none of them focused on the temporal-compositional evolution of the lavas erupted during, or just before, this major event, which is the object of this paper. This study focuses on trace elements, including fluid mobile and semi-volatile species (e.g., Li, B, Re, In, Cd, Tl, Bi). In particular, volatile trace metals are used to reconstruct the degassing history of this exceptional eruption, which is constrained from remote observations (Bhugwant et al., 2009; Gouhier and Coppola, 2011; Tulet and Villeneuve, 2011).

We first address the question of whether this exceptional, caldera-forming eruption was preceded by geochemical precursors. Thus, we investigate the previous eruptions of 2006 and 2007. Then, we consider the possibility that the temporal-compositional evolution of the April

\* Corresponding author.

E-mail address: I.Vlastelic@opgc.univ-bpclermont.fr (I. Vlastélic).

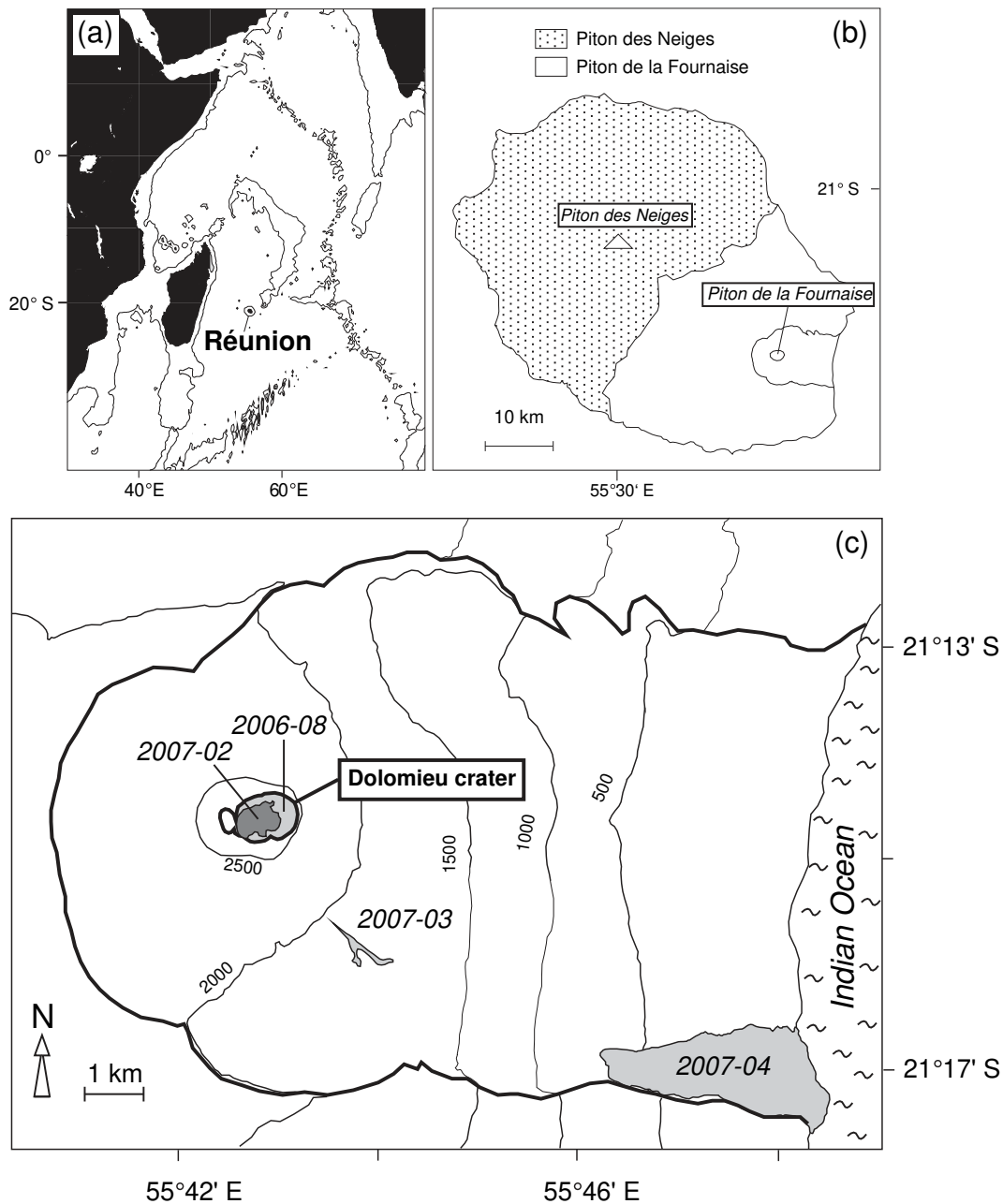


**Fig. 1.** Location maps. (a) Map of the Western Indian Ocean showing the location of Réunion Island. The 3000-m depth contour is indicated. (b) Map of Réunion Island showing the location of Piton des Neiges and Piton de la Fournaise. (c) Map of the Piton de la Fournaise volcano showing the lava flows produced during the eruptions of August–December 2006, February 2007, March 2007, and April 2007.

2007 lavas recorded the processes that affected the shallow magma reservoir shortly before, or even during, the eruption. These processes potentially include (1) pre-eruptive vapour transfer and accumulation at the top of the magma column, which could play a role in triggering major eruptions (Berlo et al., 2004; Kent et al., 2007; Rowe et al., 2008); (2) massive volatile exsolution in response to static decompression of the magma reservoir as magma drained to feed lateral eruptions (Johnson, 1992; Poland et al., 2009); (3) the rapid crystallisation of clinopyroxene and plagioclase microlites, depending on the thermal state of the shallowest magma reservoir and the dynamics of magma transfer to the eruption site (Welsch et al., 2009); and (4) magma contamination during storage. Interaction with or assimilation of oceanic crust or edifice material could occur as magma accumulates before high-flux eruptions (Vlastélic et al., 2005, 2007) or when volcanic activity resumes after a long period of quiescence, as in 1998 (Salaün et al.,

2010). The scenarios of submarine collapse (Kent et al., 1999) and hydrothermal caldera (Merle et al., 2010) also raise the possibility of the entrainment of hydrothermally altered material that may compose the interior of the volcano (Lénat et al., 2000). These different possibilities are discussed in light of the trace element data presented.

## 2. Eruptive background

The Piton de la Fournaise volcano is very frequently active, but most eruptions are of small volume and short duration. Amongst the 105 eruptions estimated to have occurred between 1920 and 2007 (Stieltjes and Moutou, 1989; Peltier et al., 2009a), only four produced more than  $50 \times 10^6 \text{ m}^3$  of lava, and only two more than  $100 \times 10^6 \text{ m}^3$ . These two most voluminous eruptions (July 1931 and April 2007) caused major summit collapses. Unlike in 1931, the eruptive history

**Table 1**  
Major-trace element concentrations of Piton de la Fournaise lavas erupted between August 2006 and April 2007.

	Reference standard		August 2006								
Sample name	BHVO-2 <sup>(1)</sup>	2 $\sigma$ (%) <sup>(2)</sup>	0608-302	0608-302 dup	0608-311	0609-131	0609-281	0610-111	0610-261	0611-142	0612-111
Eruption date (d/m/y)			30/08/06		31/08/06	13/09/06	28/09/06	11/10/06	26/10/06	14/11/06	12/12/06
Sample type			SSB		SSB						
					q	q	q	q	q	q	q
SiO <sub>2</sub>			49.97		49.50						
Al <sub>2</sub> O <sub>3</sub>			14.23		14.20						
Fe <sub>2</sub> O <sub>3</sub>			12.73		11.97						
MgO			7.22		6.84						
CaO			11.89		11.21						
Na <sub>2</sub> O			2.65		2.80						
K <sub>2</sub> O			0.71		0.75						
TiO <sub>2</sub>			2.72		2.59						
MnO			0.17		0.16						
P <sub>2</sub> O <sub>5</sub>			0.32		0.31						
Li	4.8	5.6	5.86	5.83	5.88	5.83	5.90	5.80	5.83	5.81	5.87
Be	1	11.3	1.06	1.04	1.10	1.03	1.09	1.07	1.08	1.06	1.08
B <sup>(3)</sup>	2.76*	11.5	2.67								
Sc	32	2.7	33.4	33.1	34.2	33.2	33.5	33.3	33.9	33.4	33.2
Ti	16300	3.7	16026	15888	16256	15930	16076	16068	16269	16028	16033
V	317	2.2	306	305	314	306	309	306	311	306	308
Cr	280	6.8	244	245	250	240	242	237	239	239	246
Co	45	2.3	45.6	44.9	46.0	44.9	45.3	45.2	46.0	45.3	45.8
Ni	119	6.0	92.2	90.7	90.8	87.9	88.8	85.8	88.2	87.1	88.9
Cu	127	2.8	109	107	110	108	109	109	111	109	109
As	0.92*	26.4	0.84	0.79	0.80	0.79	0.75	0.80	0.82	0.84	0.79
Rb	9.11	4.0	17.4	17.4	17.4	17.4	17.4	17.5	17.4	17.4	17.3
Sr	396	6.3	354	356	352	354	353	355	354	352	352
Y	26	7.1	29.3	28.5	28.9	28.8	28.3	28.5	28.6	28.9	29.1
Zr	172	8.3	193	193	193	193	191	192	193	192	192
Nb	18.1	4.0	21.9	21.9	22.1	22.0	22.0	22.1	22.1	22.0	21.9
Mo	3.4*	38.3	0.9	1.2	1.0	1.5	1.2	1.8	1.1	1.0	1.0
Cd	0.12*	8.6	0.130	0.132	0.138	0.132	0.122	0.133	0.129	0.114	0.121
In	0.087*	3.9	0.090	0.087	0.085	0.090	0.086	0.085	0.085	0.085	0.086
Sn	1.69*	4.1	1.70	1.70	1.74	1.74	1.66	1.73	1.71	1.70	1.71
Sb	0.095*	8.9	0.063	0.059	0.070	0.065	0.061	0.068	0.070	0.071	0.067
Cs	0.1	6.2	0.267	0.259	0.268	0.262	0.270	0.261	0.265	0.263	0.268
Ba	131	4.2	135	136	136	136	135	136	135	135	136
La	15.2	5.6	19.4	18.6	19.4	19.5	19.3	19.5	19.5	19.4	19.4
Ce	37.5	6.0	44.3	44.2	44.2	44.8	44.2	44.2	44.2	44.3	43.9
Pr	5.35	5.9	5.91	5.92	5.92	5.94	5.86	5.93	5.91	5.91	5.91
Nd	24.5	4.8	25.9	25.9	25.9	26.1	26.0	26.0	25.9	25.9	25.9
Sm	6.07	5.2	6.22	6.22	6.33	6.29	6.20	6.26	6.23	6.27	6.30
Eu	2.07	5.2	2.09	2.11	2.10	2.09	2.07	2.09	2.10	2.07	2.10
Tb	0.92	6.1	0.960	0.963	0.973	0.971	0.970	0.970	0.964	0.969	0.978
Gd	6.24	5.3	6.47	6.50	6.47	6.53	6.40	6.53	6.46	6.47	6.50
Dy	5.31	5.4	5.63	5.65	5.63	5.67	5.58	5.68	5.63	5.63	5.71
Ho	0.98	7.3	1.04	1.06	1.06	1.06	1.04	1.06	1.06	1.06	1.06
Er	2.54	4.8	2.75	2.76	2.77	2.78	2.71	2.77	2.75	2.75	2.77
Tm	0.33	6.4	0.361	0.358	0.363	0.361	0.360	0.359	0.362	0.359	0.364
Yb	2	5.5	2.20	2.21	2.23	2.21	2.18	2.23	2.22	2.20	2.22
Lu	0.274	6.0	0.299	0.306	0.306	0.303	0.308	0.305	0.300	0.302	0.309
Hf	4.36	4.9	4.69	4.67	4.64	4.72	4.67	4.69	4.67	4.69	4.69
Ta	1.14	5.1	1.37	1.38	1.38	1.38	1.37	1.37	1.37	1.37	1.38
W	0.21	3.9	0.288	0.286	0.293	0.296	0.295	0.296	0.291	0.291	0.301
Re (ppt) <sup>(3)</sup>	-	-	805								
Tl	0.026*	3.3	0.065	0.066	0.045	0.044	0.040	0.043	0.044	0.042	0.041
Pb	1.56*	14.8	1.70	1.60	1.71	1.73	1.73	1.70	1.70	1.67	1.70
Bi	0.018*	10.9	0.020	0.020	0.021	0.022	0.012	0.020	0.019	0.012	0.016
Th	1.22	5.7	2.21	2.22	2.22	2.24	2.24	2.24	2.23	2.22	2.23
U	0.403	6.0	0.555	0.551	0.552	0.560	0.565	0.569	0.554	0.559	0.553

Major element concentrations are in wt.% (XRF data acquired at Laboratoire GéoSciences Réunion).

Trace element concentrations are in ppm, with the exception of Re (in ppt).

SSB: Steady State Basalt; Oceanite: basalt with cumulative olivine (MgO > 20 wt.%).

q: quenched.

(1) BHVO-2 concentration data used as reference (from GEOREM data base, at <http://georem.mpch-mainz.gwdg.de/>). Lead and non-conventional elements (\*) were determined in this study. See text for more details.

(2) 2 $\sigma$  reproducibility on BHVO-2 (9 analyses). The low reproducibility of Pb (and possibly Mo and As) concentrations may reflect the heterogeneity of BHVO-2 powder (see Chauvel et al., 2010).

(3) Isotope dilution data. BHVO-2 was not analysed for Re. The uncertainty of Re data is 1%, as inferred from replicate analyses of Piton de la Fournaise basalts (Schiano et al., 2012).

August 2006	February 2007		March 2007	April 2007						
0612-281	0702-18-2	0702-18-3	070331-1b	070402-1	070402-1	070402-1b	070403-b	070403-b	070404-b	070404-b
28/12/06	18/02/07	18/02/07	30/03/07	TS pwd 02/04/07	TS chip 02/04/07	02/04/07	03/04/07	dup	04/04/07	dup
SSB q	SSB	SSB	SSB	SSB	SSB	pm SSB	SSB		SSB	
	48.92	48.86	48.89			48.54	48.83		48.88	
	13.98	13.88	13.82			13.62	13.65		13.7	
	12.59	12.70	12.51			12.51	12.738		12.71	
	6.69	7.03	7.12			7.32	7.5		7.34	
	11.19	11.12	11.10			10.88	11.04		11.1	
	2.48	2.44	2.44			2.26	2.37		2.54	
	0.66	0.64	0.64			0.62	0.67		0.7	
	2.66	2.64	2.64			2.61	2.61		2.62	
	0.17	0.17	0.17			0.17	0.17		0.17	
	0.30	0.29	0.29			0.29	0.3		0.3	
5.80	6.04	5.85	5.57	4.63	4.13	4.90	5.20	5.22	5.24	5.47
1.05	1.07	1.07	0.93	0.93	1.02	0.96	0.91	1.05	0.93	0.86
2.67	3.22	2.96	2.59	2.64		2.72	2.67		2.85	
33.3	33.3	33.4	32.5	32.5	33.0	32.6	32.4	32.5	32.5	33.6
15917	15928	15913	15511	15695	15822	15705	15607	15701	15528	16115
305	305	306	296	280	299	298	298	294	297	304
245	238	266	262	277	286	275	270	278	281	298
45.7	45.3	47.4	46.7	47.5	49.4	47.8	47.8	48.5	48.3	49.7
89.0	83.0	102.7	94.5	102	109	103	104	105	110	113
109	107	107	105	94.3	83.2	100	106	107	100	103
0.81	0.79	0.79	0.72	0.79	0.75	0.84	0.79	0.76	0.72	0.76
17.3	17.2	16.7	16.5	15.9	15.9	16.1	16.4	16.6	16.4	17.1
354	351	343	342	334	332	334	340	345	336	349
28.9	29.1	29.0	27.92	27.7	27.8	28.0	28.0	28.5	27.8	28.8
192	192	188	185	185	186	185	186	188	184	193
21.8	21.6	21.2	20.70	20.6	20.6	20.7	20.6	20.8	20.4	21.3
1.0	1.3	4.8	0.9	2.1	1.4	0.8	0.9	0.9	1.0	0.9
0.130	0.131	0.142	0.131	0.133	0.133	0.132	0.151	0.165	0.164	0.154
0.088	0.089	0.085	0.09	0.086	0.089	0.088	0.096	0.092	0.122	0.130
1.71	1.70	1.72	1.65	1.65	1.65	1.67	1.69	1.71	1.86	1.92
0.063	0.065	0.072	0.05	0.059	0.056	0.052	0.054	0.063	0.054	0.055
0.267	0.262	0.262	0.23	0.227	0.240	0.229	0.235	0.256	0.233	0.225
135	134	130	127	124	123	125	127	130	125	131
19.4	19.2	18.7	18.4	18.3	18.3	18.3	18.3	18.5	18.2	19.0
44.3	43.8	42.7	41.8	41.9	42.0	41.9	42.3	42.4	41.6	43.6
5.89	5.88	5.77	5.64	5.61	5.62	5.64	5.66	5.71	5.60	5.83
25.9	25.8	25.4	24.7	24.8	24.7	24.8	24.9	25.1	24.7	25.7
6.27	6.25	6.25	6.07	6.04	6.02	6.11	6.03	6.14	6.06	6.28
2.09	2.09	2.08	2.04	2.04	2.05	2.04	2.05	2.07	2.03	2.12
0.966	0.969	0.965	0.949	0.948	0.943	0.952	0.953	0.964	0.941	0.988
6.52	6.50	6.43	6.32	6.37	6.33	6.39	6.40	6.48	6.29	6.61
5.66	5.65	5.59	5.50	5.53	5.53	5.54	5.55	5.68	5.55	5.80
1.06	1.06	1.05	1.04	1.03	1.04	1.05	1.05	1.04	1.04	1.09
2.78	2.76	2.76	2.69	2.71	2.72	2.70	2.72	2.74	2.70	2.83
0.362	0.360	0.361	0.35	0.356	0.355	0.357	0.357	0.359	0.355	0.369
2.22	2.21	2.19	2.16	2.18	2.14	2.19	2.18	2.22	2.17	2.25
0.302	0.301	0.301	0.30	0.303	0.301	0.298	0.298	0.305	0.299	0.306
4.71	4.69	4.59	4.56	4.57	4.56	4.53	4.60	4.56	4.55	4.69
1.37	1.37	1.33	1.30	1.31	1.31	1.29	1.31	1.32	1.30	1.34
0.315	0.295	0.323	0.29	0.271	0.263	0.286	0.302	0.315	0.296	0.301
1140	680	1758	802	651		657	665		878	
0.042	0.044	0.047	0.04	0.035	0.035	0.037	0.040	0.040	0.037	0.039
1.76	1.64	1.63	1.65	1.64	1.59	1.65	1.77	1.74	1.75	1.72
0.018	0.019	0.022	0.02	0.023	0.020	0.021	0.062	0.065	0.033	0.028
2.22	2.21	2.16	2.08	2.09	2.10	2.09	2.11	2.14	2.08	2.16
0.549	0.547	0.538	0.53	0.516	0.527	0.525	0.531	0.529	0.523	0.543

(continued on next page)

Table 1 (continued)

April 2007											
Sample name	070405-2	070405-2 dup	070405-1b	070406-1b	070407-1b	070408-1b	070417-1	070420-2	070420-2	070425-2	070429-1
Eruption date (d/m/y)	05/04/07		05/04/07	06/04/07	07/04/07	08/04/07	17/04/07	20/04/07	20/04/07	25/04/07	29/04/07
Sample type	Olivine-rich matrix glass	tephra matrix glass	Oceanite q	Oceanite	Oceanite	Oceanite	Oceanite	Oceanite q	matrix glass	Oceanite q	Oceanite q
SiO <sub>2</sub>			45.63	44.17	42.90	42.88	43.57	42.86		43.93	43.6
Al <sub>2</sub> O <sub>3</sub>			8.75	7.19	5.74	5.69	6.20	5.81		6.46	6.22
Fe <sub>2</sub> O <sub>3</sub>			14.15	14.40	14.93	15.01	14.97	14.86		14.998	15.018
MgO			20.98	24.77	28.94	29.19	27.94	28.71		27.56	27.94
CaO			7.10	5.80	4.62	4.56	5.03	4.70		5.26	5.06
Na <sub>2</sub> O			1.64	1.27	1.01	0.99	1.09	1.02		1.2	1.16
K <sub>2</sub> O			0.42	0.30	0.25	0.25	0.27	0.26		0.32	0.33
TiO <sub>2</sub>			1.67	1.38	1.09	1.07	1.17	1.09		1.21	1.16
MnO			0.18	0.19	0.19	0.19	0.19	0.19		0.19	0.19
P <sub>2</sub> O <sub>5</sub>			0.18	0.15	0.11	0.11	0.13	0.11		0.13	0.13
Li	4.81	4.60	3.92	3.87	3.47	3.33	3.38	3.37	5.49	3.26	3.32
Be	0.72	0.69	0.57	0.55	0.43	0.40	0.46	0.42	0.93	0.39	0.41
B <sup>(3)</sup>			1.62	1.47	1.20	1.15	1.56	1.42			1.39
Sc	29.8	27.8	20.2	17.1	16.4	16.1	17.5	16.1	32.1	15.4	15.9
Ti	14861	14022	9242	9107	6886	6591	7595	6792	15293	6304	6686
V	265	249	177	168	133	129	148	133	291	125	131
Cr	441	402	844	809	981	1090	1257	1327	584	1343	1196
Co	51.9	49.4	103	104	123	123	184	172	49.8	174	162
Ni	182	180	902	930	1164	1178	1078	1149	204	1197	1154
Cu	97	91	64.16	60.6	47.1	44.9	48.9	45.6	103	42.0	44.1
As	0.86	0.72	0.46	0.44	0.38	0.32	0.41	0.38	0.77	0.33	0.35
Rb	13.5	12.9	8.81	8.20	6.67	6.35	7.54	6.65	16.1	6.27	6.75
Sr	296	281	195	184	143	137	160	143	333	134	143
Y	25.7	24.5	16.7	16.2	12.0	11.5	13.0	11.6	27.2	10.8	11.5
Zr	167	158	107	103	79	76	87	78	181	72	77
Nb	17.2	16.5	11.11	10.39	8.39	7.95	9.61	8.50	20.3	8.01	8.58
Mo	0.9	0.8	0.7	0.6	0.5	0.5			1.0		
Cd	0.112	0.105	0.081	0.079	0.057	0.060	0.068	0.060	0.124	0.055	0.060
In	0.079	0.078	0.055	0.053	0.040	0.041	0.045	0.040	0.084	0.038	0.039
Sn	1.66	1.51	0.979	0.958	0.708	0.678	0.765	0.692	1.63	0.700	0.730
Sb	0.047	0.044	0.033	0.033	0.024	0.024	0.031	0.029	0.049	0.024	0.029
Cs	0.183	0.176	0.136	0.128	0.103	0.101	0.117	0.101	0.231	0.096	0.103
Ba	107	102	68.4	64.1	52.0	50.5	58.4	51.7	124	48.6	52.3
La	15.5	14.9	9.90	9.28	7.43	7.12	8.39	7.45	18.0	7.00	7.50
Ce	35.9	34.5	23.1	21.7	17.9	17.1	19.4	18.0	41.0	16.8	18.0
Pr	4.87	4.67	3.12	2.94	2.31	2.23	2.59	2.31	5.54	2.16	2.30
Nd	21.8	20.9	13.9	13.2	10.2	9.78	11.3	10.1	24.3	9.48	10.1
Sm	5.55	5.29	3.44	3.35	2.50	2.43	2.76	2.48	5.91	2.30	2.48
Eu	1.90	1.83	1.18	1.15	0.86	0.82	0.94	0.84	2.00	0.78	0.83
Tb	0.903	0.864	0.559	0.541	0.400	0.388	0.441	0.393	0.935	0.366	0.384
Gd	5.96	5.74	3.74	3.61	2.68	2.58	2.93	2.61	6.19	2.45	2.59
Dy	5.28	5.07	3.26	3.18	2.33	2.25	2.56	2.31	5.42	2.12	2.26
Ho	0.99	0.95	0.608	0.590	0.439	0.421	0.475	0.427	1.01	0.399	0.420
Er	2.57	2.46	1.59	1.55	1.14	1.11	1.24	1.12	2.63	1.04	1.12
Tm	0.335	0.322	0.208	0.203	0.149	0.147	0.164	0.148	0.346	0.138	0.145
Yb	2.05	1.97	1.28	1.26	0.925	0.903	1.02	0.912	2.11	0.860	0.894
Lu	0.283	0.271	0.178	0.173	0.132	0.126	0.141	0.127	0.292	0.119	0.125
Hf	4.18	4.03	2.61	2.52	1.89	1.83	2.10	1.89	4.48	1.76	1.87
Ta	1.11	1.07	0.709	0.669	0.533	0.514					
W	0.232	0.223	0.153	0.146	0.133	0.177					
Re (ppt) <sup>(3)</sup>			490			214					
Tl	0.034	0.034	0.023	0.020	0.018	0.018	0.018	0.017	0.041	0.016	0.018
Pb	1.41	1.35	0.831	0.757	0.614	0.586	0.672	0.612	1.62	0.572	0.641
Bi	0.013	0.013	0.011	0.013	0.011	0.009	0.010	0.008	0.018	0.007	0.009
Th	1.79	1.72	1.14	1.06	0.853	0.836	0.986	0.879	2.060	0.822	0.887
U	0.451	0.430	0.285	0.270	0.217	0.211	0.244	0.221	0.512	0.207	0.220

prior to the April 2007 eruption is known in great detail, especially since 1972. This recent history is first marked by an unusually long quiet period, between 1992 and 1998, which ended with a no-less unusual long eruption (March–September 1998). This eruption led to the suggestion that the volcano had entered a new, major eruptive sequence in 1998 (Staudacher et al., 2001). Perhaps more importantly, the behaviour of the plumbing system changed markedly in 2000, as evidenced by the reappearance of olivine-rich lavas after more than 20 years of absence. From 2000, the volcano also showed repeated short-term eruptive cycles, each being characterised by (1) decreasing elevation of the eruptive vents, (2) increasing abundance in cumulative olivine, (3) summit inflation and (4) deepening of dyke roots (Peltier et al., 2008). Based on these criteria, Peltier et al. (2009a) identified five cycles between the end of 2000 and April 2007 (end of 2000–January 2002, November 2002–January 2004, May 2004–February 2005, October 2005–December 2005 and July 2006–April 2007). To explain the change of eruptive regime in 2000, the authors also proposed that magma recharge and the drainage of the shallow reservoir were balanced before 2000. After 2000, the increasing magma flux from the depth possibly led to magma accumulation at shallow depths. Since 2007, the volcanic activity progressively vanished (very small eruptions occurred between 2008 and 2010, and no eruption occurred in 2011 and 2012).

### 3. The July 2006–April 2007 eruptive cycle

The sequence of events that led to the April 2007 paroxysmal activity started in July 2006. Following a modest eruption in July ( $2.8 \times 10^6 \text{ m}^3$ ), a four-month long eruption (August 30, 2006 to January 1, 2007) filled the Dolomieu Crater with circa  $20 \times 10^6 \text{ m}^3$  of lava. The summit eruptive activity resumed briefly in February 18, 2007 ( $<10^6 \text{ m}^3$ ). As the volcano continued to inflate, an eruption occurred on March 30 at 1900 m along the south-east flank and produced again a small volume of lava ( $<10^6 \text{ m}^3$ ). The subsequent April events are described in detail by Staudacher et al. (2009), Michon et al. (2007) and Peltier et al. (2009b). Briefly, the eruption started on April 2, at 590 m above sea level (asl), 7 km away from the summit along the south-east rift zone (Fig. 1c). The seismic tremor, the thermal anomaly, and the height of lava fountains all indicated that the rate of magma production increased drastically until the summit Dolomieu crater collapsed in the night of the 5 to 6 April, forming a caldera of  $90 \times 10^6 \text{ m}^3$ . Staudacher et al. (2009) noted that the maximum tremor occurred during the day of April 6, 12 to 24 hours after the main collapse event. Following the paroxysmal phase, the eruption continued at this more or less regular, but elevated, rate until May 1. The total volume of lava produced, initially estimated to be approximately  $130 \times 10^6 \text{ m}^3$  (Staudacher et al., 2009), has been re-evaluated to be  $240 \times 10^6 \text{ m}^3$ . The eruption rate was  $52 \text{ m}^3/\text{s}$  on average but most likely exceeded  $200 \text{ m}^3/\text{s}$  during the paroxysmal phase. Thermal monitoring from space revealed that the magma output rate increased from 55 to  $75 \text{ m}^3/\text{s}$  between April 3 and 4 (Coppola et al., 2009). These rates are typically one order of magnitude higher than those estimated for normal eruptions. Based on the satellite data, the degassing paroxysm ( $1800 \text{ kg/s}$  of  $\text{SO}_2$ ) occurred in the morning of April 6 (Tulet and Villeneuve, 2011). Summit emanations during collapse exceeded those expected from lava effusion, possibly as a result of opening of the hydrothermal system (Gouhier and Coppola, 2011). The summit collapse was ascribed to a sub-surface pressure drop caused by rapid, lateral withdrawal of magma from the shallow reservoir (Staudacher et al., 2009).

The lavas emitted until April 4, 2007 are poorly phyric transitional basalts with little compositional variability, often referred to as steady-state basalts. The amount of olivine crystals increased drastically between April 4 and 5 (one day before the summit collapse) and remained elevated ( $\geq 50 \text{ wt.}\%$ ) until the end of the eruption. Because no geochemical study focused on this period, chemical data are

sparse. Naturally quenched samples (Pél e's hairs) from the early stage of the April 2007 eruption show melt compositions (MgO up to 8.6 wt.%) amongst the most primitive ever measured at Piton de la Fournaise (Villemant et al., 2009). The Pb isotopic compositions of April 2007 lavas are indistinguishable from previous eruptions (2005–2007), with the exception of an unradiogenic anomaly (April 5) coinciding with the paroxysmal phase of the eruption (Vlast el ic et al., 2009).

### 4. Methods

Lava samples were collected during the course of the eruptions. Some were quenched in deionised water (see Table 1). The major element concentrations were measured on fused beads by X-ray fluorescence (XRF) spectrometry at Laboratoire G eoSciences R union. A subset of samples was analysed for the total S, Cl, F and  $\text{H}_2\text{O}$  (Service d'Analyse des Roches et Min eraux, CRPG, Nancy). Sulphur converted to  $\text{SO}_2$  was measured by IR spectrometry. The water content was determined by volumetric Karl Fisher titration. The chlorine content was determined by a spectrophotometric method based on the formation of ferrithiocyanate, and the F content was determined by potentiometry using an ion-selective electrode (Vernet et al., 1987). Trace element analyses were performed on powders made by crushing rock chips in an agate mortar. Handpicked chips, including interstitial glass from an olivine-rich sample (070420-2) and P el e's hairs and tears (070405-2), were also analysed. The boron concentration was determined using the new direct isotope dilution method of Menard et al. (submitted), where the B isotopic compositions of HF-digested rocks are measured by ICPMS without any evaporation step. The rhenium concentration was measured by isotope dilution and ICPMS following the method described in Schiano et al. (2012). Other trace elements were measured more classically using external calibration. Approximately 100 mg of the sample were dissolved in 2 ml of 28 M HF and 1 ml of 14 M  $\text{HNO}_3$  in a savillex beaker for 36 hours at  $70^\circ \text{C}$ . The solutions were evaporated to near dryness at  $65^\circ \text{C}$  (to prevent the loss of the volatile fluoride species, such as  $\text{AsF}_3$ ). After the addition of a few ml of 7 M  $\text{HNO}_3$ , solutions were evaporated to near dryness, and clear solutions were obtained by adding 20 g of 7 M  $\text{HNO}_3$ . These solutions were diluted with deionised water by a factor of 20 to 10 to reach rock dilution factors ranging from 4000 to 2000. The trace element abundances were determined by quadrupole ICPMS (Agilent 7500, Laboratoire Magmas et Volcans). Given the instrumental detection limit of typically 1 ppt, it is possible to analyse elements that are present at the ppb level in rocks (e.g., Bi, Tl, Cd). The analyses were performed in plasma robust mode (1550 W). The reaction cell (He mode) was used to reduce interferences on masses ranging from 45 (Sc) to 75 (As). The signal was calibrated externally (every 4 samples) with a reference basaltic standard (USGS BHVO-2, batch 759) dissolved as samples and using the GeoRem recommended values (<http://georem.mpch-mainz.gwdg.de/>). The BHVO-2 standard was used because the trace element contents are very similar to those of R union basalts. For elements that are not well characterised (As, Mo, Sb, Sn, Cd, In, Bi, Tl), or which obviously show heterogeneity (e.g., Pb) in BHVO-2 powder (Chauvel et al., 2010), the signal was calibrated using the certified concentrations of a synthetic standard, which was also repeatedly measured. The concentrations of non-conventional elements obtained for the BHVO-2 standard are listed in Table 1 instead of the GeoRem information values. The values generally agree well with previously published values except for Cd (0.12 against 0.06 ppm). Samples were measured in a random order, and most solutions were measured twice. The external reproducibility ( $2\sigma$  error) of the method, as estimated by repeatedly dissolving and analysing BHVO-2 as an unknown, is  $<9\%$  for most elements, 11% for Be, B and Bi, 15% for Pb, 26% for As and 38% for Mo (Table 1). The low reproducibility of Pb, and possibly As and Mo, could reflect the heterogeneity of the BHVO-2 powder. Because of error correlation during the ICP-MS

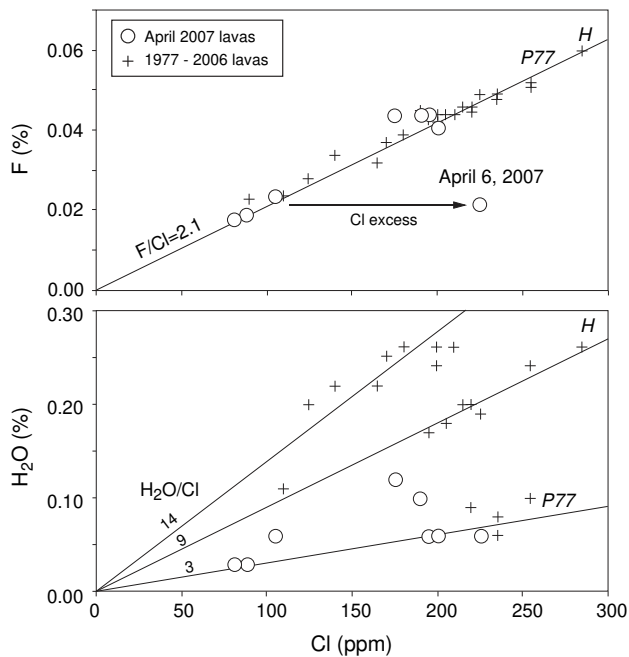


**Fig. 2.** Variations of Cl, F and H<sub>2</sub>O concentrations in recent lavas (1977–2007) of Piton de la Fournaise. Data are from Supplementary Table A. “P77” designates a pumice (77-14) erupted in 1977. The lava from April 6, 2007, has excess Cl.

measurement (instrumental drift affecting similarly different masses), the precision of the trace element ratios is often better than the precision of the concentration data, which is especially true for ratios involving elements belonging to the same family and/or with small differences of atomic masses. For instance, the precision ( $2\sigma$  error) of the La/Sm, Nb/Zr and Bi/Cd ratios are better than 2%, 5% and 10%, respectively. The accuracy of the method was checked by measuring different standards (BCR-2, BIR and BEN). For most elements, the differences with respect to recommended values were less than 20%. Chemistry blanks were systematically checked and were found to be negligible compared to the natural abundances of elements in lava samples.

## 5. Results

### 5.1. Volatile and semi-volatile element systematics in Piton de la Fournaise lavas (1977–2010)

Whole-rock S, Cl, F and H<sub>2</sub>O concentrations of recent (1977–2007) basalts of Piton de la Fournaise (Supplementary Table A) do not exceed 400 ppm, 285 ppm, 600 ppm and 0.26%, respectively. Sulphur and H<sub>2</sub>O are much less abundant than in melt inclusions (1000–2000 ppm and ca. 1%, respectively (Bureau et al., 1999)), indicating that the lavas are extensively degassed with respect to major volatile species. The lowest F and Cl concentrations are found in the olivine-rich samples while the highest concentrations are found in the 1998 Hudson lava (986–115) and in the 1977 pumice (77-14) (Fig. 2). The F/Cl ratio is constant at 2.1, except for one sample erupted on April 6, 2007, which has excess Cl. In contrast, H<sub>2</sub>O/Cl varies widely between 2.6 and 16. The April 2007 eruption displays amongst the lowest H<sub>2</sub>O/Cl ratios.

Trace element data are reported in Table 1 (2006 and 2007 eruptions) and Supplementary Table B (1977 to 2010 eruptions). The boron data for the 1977 to 2010 eruptions are reported in Menard et al. (submitted). Too few samples have been analysed for both major

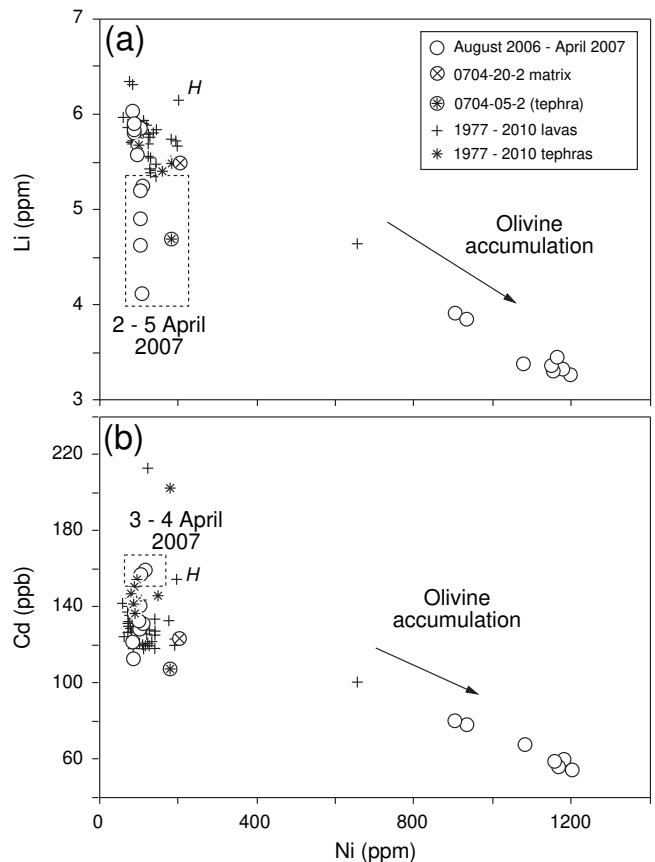


**Fig. 3.** Li and Cd versus Ni. Li and Cd are both incompatible in olivine, and both decrease with Ni (a proxy for olivine accumulation). These plots show the Li depletion and the Cd enrichment of the early stage lavas of the April 2007 eruption. The slopes of the Li–Ni and Cd–Ni arrays are used to correct whole-rock Li and Cd concentrations for the influence of olivine accumulation (see Figs. 5 and 6).

gaseous species (S, Cl, F and H<sub>2</sub>O) and semi-volatile elements to infer any robust relationship between the two types of data. All semi-volatile elements investigated in this study (Li, B, As, Cu, Sn, Sb, In, Cd, W, Re, Pb, Bi, Tl) decrease with Ni, indicating that all are incompatible in olivine (Fig. 3). However, unlike non-volatile elements, they show large variations at a given Ni content. According to the composition of the high-temperature (400 °C) gas sublimates (Vlastélic et al., 2011), Cd, Bi, and Tl are the most volatile trace elements at Piton de la Fournaise. These elements are enriched in tephtras and a few lava samples (e.g., the 1998 Hudson lava, and lavas from the early stage of the April 2007 eruption). Lithium and B as well as Cu, In and Sn have a more complex behaviour, in particular during the April 2007 eruption where they show both transient enrichments or depletions.

The relationships between Bi, Tl, In and Cd are investigated in more detail in Fig. 4. Given that Bi and Tl are respectively slightly less and slightly more volatile than Cd at Piton de la Fournaise (Vlastélic et al., 2011), the lavas have slightly higher Bi/Cd and slightly lower Tl/Cd compared to the gas sublimates. Because In is markedly less volatile than Cd, In/Cd in lavas is much higher than in the gas phase. Artificially quenched lavas do not display a distinctive Bi–Cd–In–Tl signature compared to lavas that were sampled after cooling, suggesting that late-stage degassing is not significant for these elements. However, naturally quenched samples (Pélé’s hairs and tears, ashes), the 1977 pumice, and the 1998 Hudson lava generally have elevated Bi/Cd and Bi/Tl ratios and low In/Cd and In/Tl ratios, while Tl/Cd is not significantly different from common lavas (with the possible exception of Hudson lava with a clear

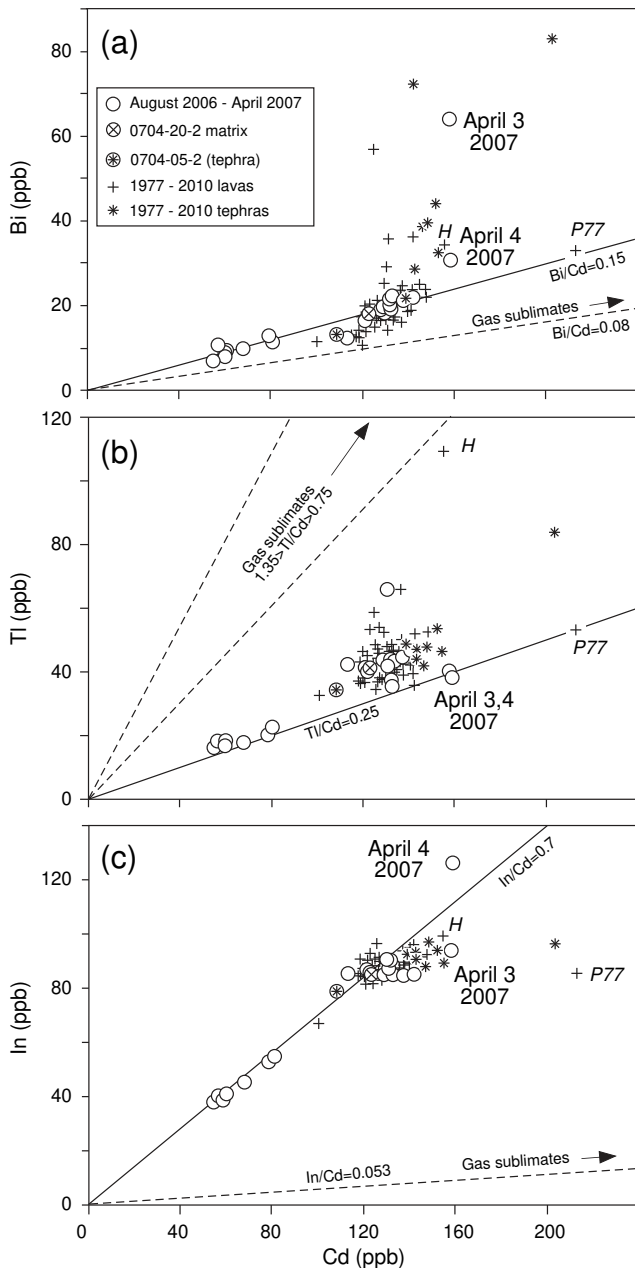


**Fig. 4.** Bi–Tl–In–Cd covariations in recent lavas (1977–2010) of Piton de la Fournaise. Data are from Table 1 (August 2006 to April 2007 eruptions) and Supplementary Table B (other eruptions). “H” designates the Hudson lava erupted in March 1998. “P77” designates a pumice (77-14) erupted in 1977. Arrows point toward the composition of high temperature (400 °C) gas sublimates from Piton de la Fournaise (Vlastélic et al., 2011).

Tl enrichment). The excess of Bi in these samples is not consistent with the incorporation of gas sublimates.

## 5.2. The 2006–2007 time evolution

The lavas erupted between July 2006 and March 2007 show little compositional variation, most trace element variations being within analytical error (Table 1 and (Vlastélic et al., 2007)). The exceptions are spikes in some volatile trace elements. Thallium is elevated in the first lavas of the August–December 2006 eruption (66 ppb against 40–45 ppb in subsequent lavas). Molybdenum and rhenium are both enriched (by a factor of two at least) in sample 0702-18-3 from

February 2007. Such coupled enrichments suggest the occurrence of rhenian molybdenite ((Mo,Re) $S_2$ ), a gas sublimate mineral that has been essentially described at the Kudryavy volcano, Kurile Islands, Russia (Tessalina et al., 2008). The following activity, in April 2007, is first marked by a transition from steady-state basalts to olivine-rich basalts between April 4 and 5. This event is recorded in whole-rock compositions by a drastic increase in the concentration of elements that are compatible in olivine (Ni, Co and Cr) (Fig. 5) and a corresponding decrease in moderately (e.g., Yb, Li) to highly (e.g., La, Th, Nb) incompatible elements. A detailed inspection of Ni (or La) temporal trend reveals that the transition was initiated as early as February 2007. The tight negative correlations between Ni and refractory incompatible elements (not shown) indicate that olivine accumulation is the cause of much of the chemical variability seen in whole-rock samples and thus that the melt composition changed little over that period. The interstitial glasses from the olivine-rich tephra (070405-2) and the oceanite sample 0704-20-2 have similar compositions as steady-state basalts, although with higher Ni (180–200 ppm against 90–110 ppm) and lower incompatible element contents. This difference may reflect either a more primitive composition or the occurrence of very small olivine crystals in the handpicked silicate glass. The features described above are rather common for Piton de la Fournaise, however. The April 2007 eruption stands out from previous eruptions in showing chemical anomalies that occurred successively during the first few days of the eruption.

- (1) Semi-volatile elements display anomalous behaviours between April 2 and 6. On the one hand, Li, Cu and Tl show low concentrations that cannot be explained by olivine accumulation (Figs. 3a and 5). Menard et al. (submitted) also note that these early stage lavas have abnormally low B/Nb ratios. The most pronounced depletion is found in the first lavas erupted on April 2 (by a factor of 0.70, 0.76 and 0.82 for Li, Cu, and Tl, respectively, taking for reference the average composition of 2006 eruptions). The interstitial glass from the olivine-rich tephra produced on April 5 is also depleted in Li and Cu, even when its higher Ni content is taken into account (Fig. 3a). These observations agree with the recent identification of Cu depletion in olivine-hosted melt inclusions from the same eruption (Collins et al., 2012). Coupled Li–Cu anomalies, including both enrichments and depletions, were previously described in phenocrysts (plagioclase and amphibole) from the early stages of paroxysmal eruptions of Mount St. Helens (Berlo et al., 2004; Kent et al., 2007; Rowe et al., 2008). It is noteworthy that the April 2007 samples depleted in Li show Li isotopic compositions ( $4.0 < \delta^7\text{Li} < 4.5\%$ ) that are slightly heavier than the average signature of steady-state basalts ( $\delta^7\text{Li} = 3.6 \pm 0.4$  (1 $\sigma$ ),  $n = 27$  (Vlastélic et al., 2011)), although the difference is barely significant. On the other hand, Bi, Cd, In and Sn are enriched (by a factor of 1.85, 1.23, 1.28 and 1.10, respectively) during the same period (Figs. 3b and 6), although there is a short (1–2 days) time offset between the Li–Cu depletion (mostly on April 2) and the Bi–Cd–In–Sn enrichment (April 3 and 4). Such enrichment does not seem to occur for Tl, Pb, As, Re and B. In detail, Bi, Cd, In and Sn show contrasting responses over these two days, the Bi concentration increasing first (dominant anomaly on April 3), followed by Cd (similar anomalies on April 3 and 4) and In–Sn (anomaly on April 4). The samples from April 3 and 4 have thus anomalously high Bi/Cd and In/Cd ratios, respectively (Fig. 4). A chlorine excess occurred slightly later, during the eruption paroxysm on April 6 (Fig. 2). The chlorine most likely originates from the huge steam plume that formed when the lava flow entered the sea (Staudacher et al., 2009).
- (2) Coinciding with the summit collapse and the eruption paroxysm (April 5 and 6), the ratios of trace elements that are more versus less incompatible (e.g., La/Sm or Nb/Zr) are anomalously low

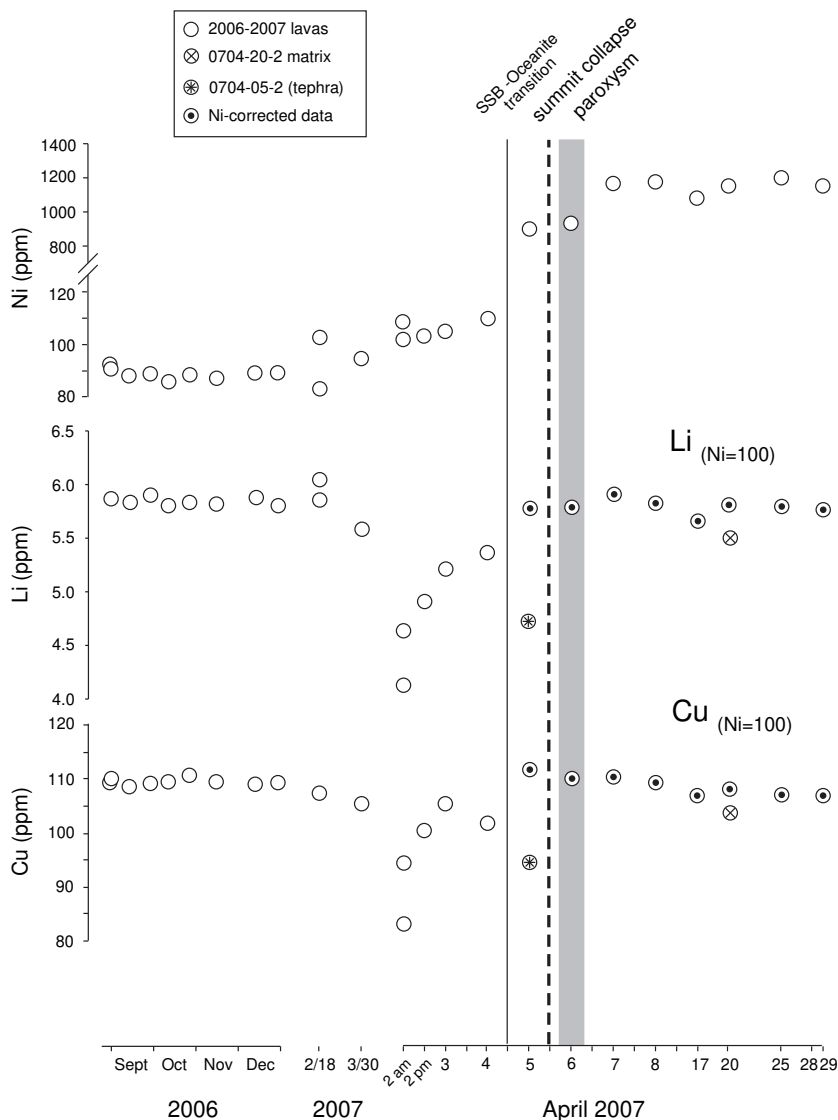


**Fig. 5.** Concentration of Ni, Li and Cu plotted versus time. Different scales of time are used along the “x” axis to emphasise the rapid chemical variations occurring during the very first days of the April 2007 eruption. The transition from steady-state basalts to olivine-rich lavas (also referred to as oceanites), the summit collapse (main event) and the eruption paroxysm (maximum tremor, highest lava fountains and degassing peak) are indicated. The lithium and Cu contents of the olivine-rich samples were corrected for olivine accumulation with 100 ppm Ni as reference:  $[X]_{Ni=100} = [X]_{sample} - S_{X-Ni} \cdot ([Ni]_{sample} - 100)$ , where  $S_{X-Ni}$  is the slope of the linear regression line through data points in X versus Ni plot.  $S_{X-Ni}$  was inferred using the data given in Table 1, removing the anomalous concentrations from the early stage of the April 2007 eruption (April 2 to 4). Slopes of  $-0.0023$  and  $-0.0593$  were calculated for Li and Cu, respectively (see also Fig. 3). Distinctive symbols are used for concentrations corrected for olivine accumulation (circle with a dark dot), for the handpicked interstitial glass from sample 0704-20-2 (circle with a cross), and for the tephra collected on April 5 (circle with a star).

(Fig. 7). On April 6, La/Sm decreases down to 2.77, which is the lowest value measured in recent lavas of Piton de la Fournaise (Vlastélic et al., 2005, 2007 and Supplementary Table B).

## 6. Discussion

The geochemical evolution of lavas in 2006 and early 2007 does not show strong precursors to the April 2007 events. The most significant signal is the trend of increasing compatible element concentration (e.g., Ni) and decreasing ratios of elements that are more versus less incompatible (e.g., La/Sm or Nb/Zr) (Figs. 5 and 7). This trend, initiated in February 2007, may reflect the increasing contribution of a less differentiated melt, which has been previously identified in April 2007 glassy samples on the basis of major elements (Villemant et al., 2009). The coincidence of a depleted trace element signature with the eruption paroxysm raises the possibility that fast rising magma undergoes limited crystallisation during its transfer to the eruption site. The following

discussion will focus on the degassing history of the April 2007 magmas as recorded by semi-volatile elements.

### 6.1. Origin of Li, Cu, and Tl depletions (April 2 to 4)

The depletion of Li, Cu and Tl in the first lavas of the April 2007 eruption is difficult to explain by crystal fractionation because no mineral, or simple mineral assemblage, contains all three elements. The entrainment or the assimilation of hydrothermally altered material is also unlikely because the samples are fresh and do not show a systematic fractionation of fluid-mobile elements (e.g., Rb, U, Pb). Instead, Li, Cu and Tl could be lost during magma degassing (Berlo et al., 2004; Kent et al., 2007; Rowe et al., 2008). However, these elements are only moderately volatile, and only a very small fraction of Li, Cu and Tl (0.02, 1 and 0.22%, respectively) is expected to ultimately leave magmas (Rubin, 1997). The observed loss, in the range of 15–30%, thus requires abnormal degassing conditions.

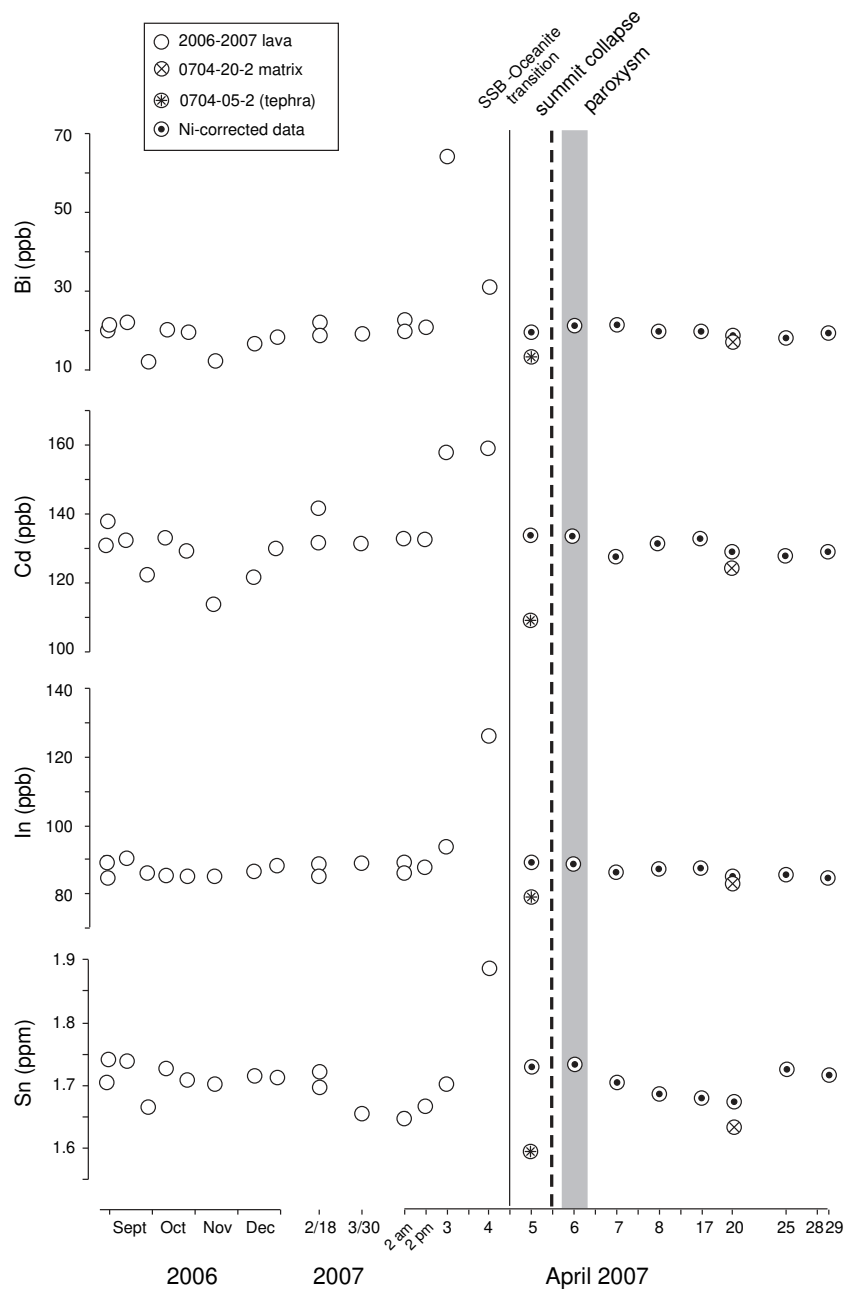


**Fig. 6.** Concentration of semi-volatile elements (Bi, Cd, In, Sn) plotted versus time. Bi, Cd, In and Sn contents of olivine-rich samples were corrected for olivine accumulation as described in the caption of Fig. 5, with  $S_{\text{Bi-Ni}} = -1.00 \times 10^{-5}$ ,  $S_{\text{Cd-Ni}} = -6.67 \times 10^{-5}$ ,  $S_{\text{In-Ni}} = -4.32 \times 10^{-5}$  and  $S_{\text{Sn-Ni}} = -9.35 \times 10^{-4}$ . Distinctive symbols are used for concentrations corrected for olivine accumulation (circle with a dark dot), for the handpicked interstitial glass from sample 0704-20-2 (circle with a cross), and for the tephra collected on April 5 (circle with a star).

The unique properties of Li, including a high affinity for aqueous fluids and a high diffusivity in silicate melts, raise the possibility of Li transport in a  $\text{H}_2\text{O}$ -rich phase rapidly exsolving at shallow depth. Vapour transfer may result in Li depletion at the bottom of the magma chamber and the accumulation of Li at the top (Berlo et al., 2004). The complementary enriched Li reservoir was not found in April 2007 products and could have been lost either as vapour, brines or phreatic ash during the major degassing event of the summit, between April 6 and April 14 (Gouhier and Coppola, 2011). Nevertheless, the hypothesis of a pre-eruptive exsolution of a Li-bearing aqueous phase agrees with (1) the evidence for shallow magma storage prior to the April 2007 eruption. The lack of deep pre-eruptive seismic activity, as well as the large volume of magma produced over a relatively short time-period

( $240 \times 10^6 \text{ m}^3$  in 3 weeks), suggest that the April 2007 magmas were stored approximately at the level of the main vent (590 m above sea level), where a magma reservoir was previously identified (Peltier et al., 2007). On this basis, the April 2007 eruption stands out from the previous voluminous eruption of March 1998, which sampled progressively ( $60 \times 10^6 \text{ m}^3$  in 6 months) a magma reservoir located at least 5 km below sea level (Battaglia et al., 2005). The first lavas produced in March 1998 showed no chemical anomaly, neither in Li nor in any other semi-volatile elements (Supplementary Table B). (2) It is generally recognised that, unlike  $\text{CO}_2$ , water solubility in basaltic magmas barely decreases with decreasing pressure until 200–100 MPa and decreases subsequently. Recent decompression experiments simulating magma degassing in a closed-system suggest that  $\text{H}_2\text{O}$  solubility drops at even

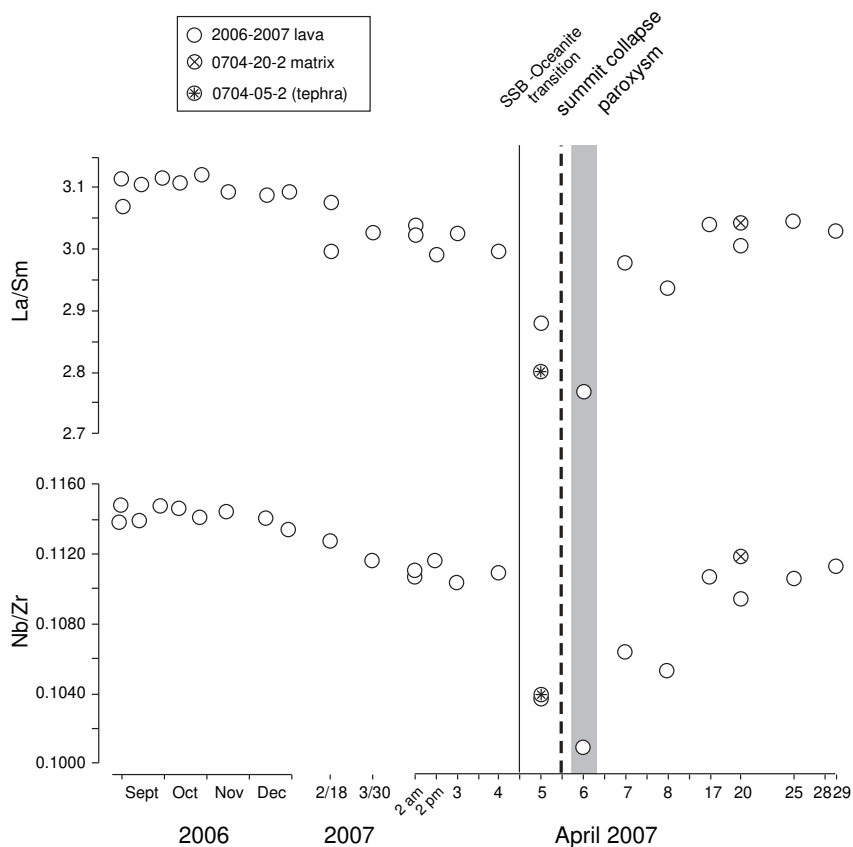


**Fig. 7.** Trace element ratios (La/Sm and Nb/Zr) plotted versus time. Distinctive symbols are used for the handpicked interstitial glass from sample 0704-20-2 (circle with a cross) and for the tephra collected on April 5 (circle with a star).

lower pressure, near 50 MPa (Lesne et al., 2011). This pressure corresponds to a basaltic column of 1800 m (with a density of 2700 kg/m<sup>3</sup>), which is approximately the depth of the shallow magma reservoir below the summit crater (2500 m above sea level). At such a shallow depth, the fluid phase is typically composed of 85% H<sub>2</sub>O, 10% CO<sub>2</sub>, and 5% S (mol%). (3) A large amount of lithium could be lost in equilibrium degassing conditions. For instance, the 2007 eruption also emitted a small volume of differentiated lava that most likely underwent closed-system degassing (Vlastelic et al., 2011). The extreme Li depletion (>90%) in these silicic differentiates suggests a vapour-melt partition coefficient of Li ( $D^{V-M}$ ) greater than 60. Koga et al. (2008) measured a Li depletion of 43% near bubbles of an experimentally degassed sample and estimated  $D^{V-M}$  up to 30.

Copper and Tl volatilise as sulphide and chloride complexes (Churakov et al., 2000). Like water solubility, sulphur solubility in melts drops at low pressure while chlorine solubility remains unchanged (Lesne et al., 2011). The partitioning of Cu and Tl in a sulphur-rich phase could thus explain why they are lost as Li. Yet, unlike H<sub>2</sub>O, S makes only a small fraction (<7 mol%) of the shallow fluid phase. Only elements with the highest affinity for gaseous sulphur are thus expected to significantly leave the magma. Considering a shallow gas phase with a H<sub>2</sub>O/S ratio of 17: the partition coefficient of Cu between sulphur vapour and magma must be 17 times that of Li between H<sub>2</sub>O vapour and magma to yield losses of similar magnitude. Collins et al. (2012) noted that Cu has less affinity for vapour than for sulphide melt, which is the dominant form of dissolved S at Réunion (Métrich et al., 2009). They suggested that Cu could be trapped in sinking sulphides prior to being lost to the gas phase. However, because melt inclusions from the April 2007 eruption are undersaturated in S, they acknowledge that S loss by degassing must also be important. Another possibility is that Cu hydrosulphide complexes that may form

in reducing conditions partition to high temperature aqueous supercritical fluids (Sun et al., 2004).

### 6.2. Origin of Bi, Cd, In and Sn enrichments (April 3 and 4)

Overlapping with the Li–Cu depletion (April 2 to 5), elevated concentrations of Bi, Cd, In and Sn occurred on April 3 and 4. Such excesses in elements that are dominantly chalcophile can either reflect the entrainment of dense sulphide melts, the incorporation of microscopic gas sublimates as lavas interact with the gas plume, the eruption of less-degassed magmas, incomplete degassing during eruption, or combinations of these different causes.

The entrainment of sulphide melts is expected to yield systematic enrichments of chalcophile elements, which is not observed. The presence of gas sublimates (minerals formed directly from the gas phase) is possible in the case of small magma products (ashes, Pele's hairs) (Moune et al., 2007) but is not expected in the case of massive lava samples such as those studied here. In addition, the incorporation of gas sublimates would decrease Bi/Cd while the opposite trend is observed (Fig. 4a). Our current understanding of the behaviour of semi-volatile elements does not allow us to distinguish degassing at depth from sub-aerial degassing. The lack of semi-volatile element enrichment in artificially quenched samples only tells us that semi-volatile elements are lost prior to the final stages of lava cooling. The variable but generally high Bi/Cd ratio that characterises tephtras appears as a fingerprint of less degassed melts (Fig. 4a). The explanation most likely lies in the difficulty of the slow diffusing Bi (Johnson and Canil, 2011) in reaching the melt-gas interface in the case of rapidly cooling samples undergoing incomplete degassing. However, the fact that some massive lava samples also display elevated Bi/Cd suggests that this signature is not only

due to the quenching rate but must also reflect to some extent the eruption of less degassed magma.

It remains unclear why Bi and Cd fractionate so much despite similar volatilities (Vlastélic et al., 2011) and why less volatile elements (In, Sn) are enriched while more volatile elements (e.g., Tl) are not. Regarding the first issue, it can be argued that Cd is a more robust tracer of magma degassing than Bi, which can be variably enriched in undegassed magmas (Norman et al., 2004). Indium and Sn are significantly less volatile than Bi and Cd at Piton de la Fournaise (Vlastélic et al., 2011), and, consistently, are not significantly enriched in tephros (Fig. 4c). The In–Sn excess in the April 4 sample is unique in the Piton de la Fournaise basalts analysed so far and requires abnormal conditions in the shallow magma reservoir just before summit collapse.

### 6.3. Kinetic fractionation of semi-volatile elements: constraints on degassing time-scales

The equilibrium partitioning of elements between melts and fluids clearly fails to explain the systematic of semi-volatile elements in April 2007 lavas. For instance, B is not depleted as Li, although B has higher emanation coefficient (Rubin, 1997). Similarly, Tl and Re are not enriched as Cd and Bi while less volatile In is. Given the short time-periods involved, kinetic (diffusive) fractionation might control the final concentration of semi-volatile elements in the lavas.

The lithium diffusivity in silicate melts, on the order of  $10^{-8.1} \text{ m}^2/\text{s}$  (Richter et al., 2003), is at least two orders of magnitude higher than that of other semi-volatile elements (Cd, Tl, Re, Bi, As, Pb), in the range of  $10^{-10.8}$ – $10^{-13.6} \text{ m}^2/\text{s}$  (MacKenzie and Canil, 2008; Johnson and Canil, 2011). Amongst the chalcophile elements, Tl diffuses much faster ( $10^{-10.8} \text{ m}^2/\text{s}$ ) than Bi ( $10^{-13.6} \text{ m}^2/\text{s}$ ) and Cd ( $10^{-12.6} \text{ m}^2/\text{s}$ ). Little is known about Cu diffusion, but Johnson and Canil (2011) observed the absence of a diffusion profile during degassing experiments.

Fig. 8 compares the diffusion length scale of elements to the half distance between gas bubbles inferred from Bubble Number Density (BND) (Toramaru, 2006; Bai et al., 2008). It is assumed that an element can leave the melt phase significantly only if it diffuses sufficiently fast to reach bubbles before they segregate. This simple statistical approach does not need to define the geometry nor the boundary conditions of the degassing system. To explain the selective degassing of Li and Tl

while preserving the elevated concentration in Cd and Bi (what happened between April 2 to 4), Li and Tl must diffuse over distances longer than the half distance between bubbles while Cd and Bi must diffuse over shorter distances. Given a typical BND of  $10^{12}/\text{m}^3$  for basalts (Bai et al., 2008), this condition is fulfilled for time scales ranging from a few minutes to a few hours (Fig. 8). Following the same reasoning, the elevated Bi/Cd observed on April 3 (and in many tephros from previous eruptions) can be explained by the preferential loss of Cd over Bi, which occurs when the bubble residence time in the melt ranges from a few hours to two days. These estimated degassing time-scales strikingly coincide with the time offsets of typically 1–2 days observed between the different chemical anomalies, strongly supporting the model of the diffusive fractionation of elements.

### 6.4. Reconciling Li–Cu depletion and Bi–Cd enrichment with the events that led to summit collapse

Two degassing scenarios may explain the early depletion in Li–Cu. (1) The very short degassing time scales estimated above raise the possibility of magmas degassing during their transport to the eruption site. According to Staudacher et al. (2009), the eruption drained a shallow magma reservoir through a 7 km long, sub-horizontal conduit. This conduit was first modelled as a  $7 \times 10^6 \text{ m}^3$  dyke (1000 m high and 1 m thick) (Staudacher et al., 2009) before interferometric data allowed the identification of a sill of comparable size that emplaced between March 30 and April 2 (Froger et al., 2010). This size of the magma conduit roughly corresponds to the volume of lava produced during the first 1–2 days of the eruption ( $4.5 \times 10^6 \text{ m}^3$  of lava being produced in 24 hours at a rate of  $52 \text{ m}^3/\text{s}$ ) and, thus, to the volume of lava showing the most depleted Li signature (April 2 and 3), which suggests that fast diffusing elements exsolved during this early, sub-horizontal channelling of magma. (2) Alternatively, depressurisation may have occurred in the shallow magma chamber in response to magma withdrawal to feed a lateral intrusion or the forthcoming eruption. As proposed for recent eruptions of Kilauea volcano, Hawaii (Johnson, 1992; Poland et al., 2009), such a static decompression event can trigger the massive exsolution of  $\text{H}_2\text{O}$  and  $\text{SO}_2$ . Lithium and Cu could have been lost at this stage. In this case, depressurisation must have occurred between March 30 and April 2.

The following Bi–Cd enrichment requires conditions that prevent magma outgassing. Transient pressurisation of the shallow magma reservoir as the overlying rock column started to collapse is one possibility. However, there is no evidence for pressurisation of the system or the onset of collapse before April 5 (Michon et al., 2011). Alternatively, the increasing rate of magma transfer on April 4 (Coppola et al., 2009) could have prevented the loss of semi-volatile elements such as Bi and Cd. Whatever the exact scenario of early degassing, the short time-scales required to fractionate Li from Cd (minutes to hours) and Cd from Bi diffusively (a few hours to two days) support the idea that the shallow magma reservoir underwent rapid pressure variations a few days before summit collapse.

## 7. Conclusion

Lavas erupted during the first few days of the April 2007 eruption show a transient depletion in Li, Cu and Tl (mostly on April 2) and an enrichment in Bi, Cd, In and Sn (on April 3 and 4). Both anomalies are ascribed to unusual degassing conditions that prevailed within the shallow magma plumbing system a few days before the summit collapse. The first anomaly could reflect the degassing of a magma intrusion that emplaced a shallow depth between March 30 and April 2 (Froger et al., 2010) and subsequently sampled on April 2. Alternatively, it could record the static decompression of the magma reservoir as magmas drained to feed the lateral intrusion or the forthcoming eruption. The second anomaly must result more or less directly from a transient pressurisation of the system, even though such an event was not

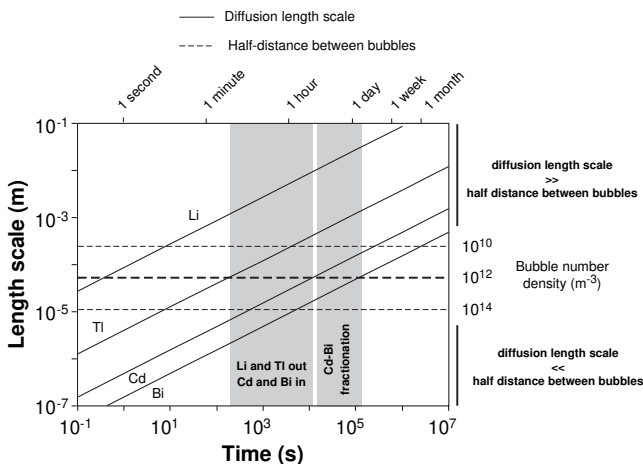


**Fig. 8.** Comparison between the diffusion length scale of elements and the half distance between gas bubbles. The diffusivity ( $D$ ) of Li, Tl, Cd, and Bi in silicate melts are  $10^{-8.1} \text{ m}^2/\text{s}$ ,  $10^{-10.8} \text{ m}^2/\text{s}$ ,  $10^{-12.6} \text{ m}^2/\text{s}$  and  $10^{-13.6} \text{ m}^2/\text{s}$ , respectively (Richter et al., 2003; Johnson and Canil, 2011). The diffusion length-scale (in metre) is given by  $(Dt)^{0.5}$ , where  $t$  is time (in second). The half distance between gas bubbles is inferred from the Bubble Number Density (BND) (Toramaru, 2006). The BND is typically  $10^{12}$  bubbles per cubic metre in basaltic melt (Bai et al., 2008). With such a BND value, the selective degassing of Li and Tl, while Cd and Bi remain in magmas, occurs for time-scales ranging from minutes to hours (grey field). The selective degassing of Cd while Bi remains in magmas occurs for degassing durations ranging from a few hours to two days (grey field).

recorded by geophysical data (Michon et al., 2011). The increasing rate of magma outflow just prior to collapse (Coppola et al., 2009) could also have prevented the loss of semi-volatile elements such as Cd and Bi.

The short, transient anomalies in the semi-volatile elements are consistent with kinetic rather than equilibrium fractionation. By comparing the diffusion length-scale of the semi-volatile elements to the distance between gas bubbles, it is estimated that the selective loss of fast diffusing elements (Li and Tl), while not mobilising slow diffusing elements (Bi and Cd), occurs for time-scales ranging from minutes to hours. Similarly, the selective enrichment of a very slowly diffusing element such as Bi, which occurred on April 3, 2007, as well as in many tephros from recent eruptions, requires degassing time-scales ranging from a few hours to two days. These very short durations are consistent with rapid changes in the shallow magma plumbing system a few days before summit collapse.

Supplementary data to this article can be found online at <http://dx.doi.org/10.1016/j.jvolgeoes.2012.12.027>.

## Acknowledgements

This paper benefited from the constructive comments of A. Kent and an anonymous reviewer. Thanks to M.J. Rutherford for handling this manuscript. The SARM (CRPG Nancy) is thanked for carrying out S, Cl, F and H<sub>2</sub>O analyses. This work benefited from the financial support from the CNRS (Institut National des Sciences de l'Univers) and the Agence Nationale de la Recherche (DEGAZMAG project, contract no. ANR 2011 Blanc SIMI 5-6 003). This study is a Laboratory of excellence *ClerVolc* contribution no 50.

## References

- Bai, L., Baker, D.R., Rivers, M., 2008. Experimental study of bubble growth in Stromboli basalt melts at 1 atm. *Earth and Planetary Science Letters* 267, 533–547.
- Battaglia, J., Ferrazzini, V., Staudacher, T., Aki, K., Cheminée, J.-L., 2005. Pre-eruptive migration of earthquakes at the Piton de la Fournaise volcano (Réunion Island). *Geophysical Journal International* 161, 549–558.
- Berlo, K., Blundy, J., Turner, S., Cashman, K., Hawkesworth, C., Black, S., 2004. Geochemical precursors to volcanic activity at Mount St. Helens, USA. *Science* 306, 1167–1169.
- Bhugwant, C., Siéja, B., Bessafi, M., Staudacher, T., Ecomier, J., 2009. Atmospheric sulfur dioxide measurements during the 2005 and 2007 eruptions of the Piton de la Fournaise volcano: implications for human health and environmental changes. *Journal of Volcanology and Geothermal Research* 184, 208–224.
- Bureau, H., Métrich, N., Semet, M., Staudacher, T., 1999. Fluid–magma decoupling in a hot-spot volcano. *Geophysical Research Letters* 23, 3501–3504.
- Chauvel, C., Bureau, S., Poggi, C., 2010. Comprehensive chemical and isotopic analyses of basalt and sediment reference materials. *Geostandards and Geoanalytical Research* 35, 125–143.
- Churakov, S.V., Tkachenko, S.I., Korzhinskii, M.A., Bochamnikov, R.E., Shmulovich, K.I., 2000. Evolution of composition of high-temperature fumarolic gases from Kudryavy Volcano, Iturup, Kuril Islands: the thermodynamic modeling. *Geochemistry International* 38, 436–451.
- Collins, S.J., Maclennan, J., Pyle, D.M., Barnes, S.J., Upton, B.G.J., 2012. Two phases of sulphide saturation in Réunion magma: evidence from cumulates. *Earth and Planetary Science Letters* 337–338, 104–113.
- Coppola, D., Piscopo, D., Staudacher, T., Cigolini, C., 2009. Lava discharge rate and effusive pattern at Piton de la Fournaise from MODIS data. *Journal of Volcanology and Geothermal Research* 184, 174–192.
- Froger, J.-L., Augier, A., Cayol, V., Souriot, T., 2010. Some considerations about the April 2007 eruption at Piton de la Fournaise suggested by InSAR data. 2010 Collapse Calderas Workshop, “Dynamics of calderas: collapse and unrest”, La Réunion, France.
- Gillot, P.-Y., Nativel, P.-E., 1989. Eruptive history of the Piton de la Fournaise volcano, Réunion Island, Indian Ocean. *Journal of Volcanology and Geothermal Research* 36, 53–65.
- Gillot, P.-Y., Lefèvre, J.-C., Nativel, P.-E., 1994. Model for the structural evolution of the volcanoes of Réunion Island. *Earth and Planetary Science Letters* 122, 291–302.
- Gouhier, M., Coppola, D., 2011. Satellite-based evidence for a large hydrothermal system at Piton de la Fournaise volcano (Réunion Island). *Geophysical Research Letters* 38, L02302. <http://dx.doi.org/10.1029/2010GL046183>.
- Johnson, D.J., 1992. Dynamics of magma storage in the summit reservoir of Kilauea Volcano, Hawaii. *Journal of Geophysical Research* 97, 1807–1820.
- Johnson, A., Canil, D., 2011. The degassing behavior of Au, Ti, As, Pb, Re, Cd and Bi from silicate liquids: experiments and applications. *Geochimica et Cosmochimica Acta* 75, 1773–1784.
- Kent, A.J.R., Clague, D.A., Honda, M., Stolper, E.M., Hutcheon, I.D., Norman, M.D., 1999. Widespread assimilation of a seawater-derived component at Loihi Seamount, Hawaii. *Geochimica et Cosmochimica Acta* 63, 2749–2761.
- Kent, A.J.R., Blundy, J., Cashman, K.V., Cooper, K.M., Donnelly, C., Pallister, J.S., Reagan, M., Rowe, M.C., Thornber, C.R., 2007. Vapor transfer prior to the October 2004 eruption of Mount St. Helens, Washington. *Geology* 35, 231–234.
- Koga, K.T., Cluzel, N., Rose-Koga, E., Laporte, D., Shimizu, N., 2008. Experimental demonstration of lithium–boron depletion during magma degassing. *Eos Transactions American Geophysical Union* 89 (53) (Fall Meet. Suppl., Abstract V31B-2143).
- Lénat, J.-F., Fitterman, D., Jackson, D.B., Labazuy, P., 2000. Geoelectrical structure of the central zone of Piton de la Fournaise volcano (Réunion). *Bulletin of Volcanology* 62, 75–89.
- Lesne, P., Kohn, S.C., Blundy, J., Witham, F., Botcharnikov, R.E., Behrens, H., 2011. Experimental simulation of closed-system degassing in the system basalt–H<sub>2</sub>O–CO<sub>2</sub>–S–Cl. *Journal of Petrology* 52, 1737–1762.
- Mackenzie, J.M., Canil, D., 2008. Volatile heavy metal mobility in silicate liquids: implications for degassing and eruption prediction. *Earth and Planetary Science Letters* 269, 488–496.
- Menard, G., Vlastélic, I., Rose-Koga, E.F., Piro, J.L., Pin, C., (submitted). High-precision determination of boron concentration in silicate rocks by Direct Isotope Dilution ICPMS: Insight into boron budget of the mantle and boron behaviour in magmatic systems, submitted to *Chemical Geology*.
- Merle, O., Barde-Cabusson, S., van Wyk de Vries, B., 2010. Hydrothermal calderas. *Bulletin of Volcanology* 72, 131–147.
- Métrich, N., Berry, A.J., O'Neill, H.S.C., Susini, J., 2009. The oxidation state of sulfur in synthetic and natural glasses determined by X-ray absorption spectroscopy. *Geochimica et Cosmochimica Acta* 73, 2382–2399.
- Michon, L., Staudacher, T., Ferrazzini, V., Bachèlery, P., Marti, J., 2007. April 2007 collapse of Piton de la Fournaise: a new example of caldera formation. *Geophysical Research Letters* 34, L21301. <http://dx.doi.org/10.1029/2007GL031248>.
- Michon, L., Massin, F., Famin, V., Ferrazzini, V., Roullet, G., 2011. Basaltic calderas: collapse dynamics, edifice deformation, and variations of magma withdrawal. *Journal of Geophysical Research* 116, B03209. <http://dx.doi.org/10.1029/2010JB007636>.
- Moune, S., Faure, F., Gauthier, P.-J., Sims, K.W.W., 2007. Pele's hairs and tears: natural probe of volcanic plume. *Journal of Volcanology and Geothermal Research* 164, 244–253.
- Norman, M.D., Garcia, M.O., Bennett, V.C., 2004. Rhenium and chalcophile elements in basaltic glasses from Ko'olau and Molokai volcanoes: magmatic outgassing and composition of the Hawaiian plume. *Geochimica et Cosmochimica Acta* 68, 3761–3777.
- Peltier, A., Staudacher, T., Bachèlery, P., 2007. Constraints on magma transfers and structures involved in the 2003 activity at Piton de la Fournaise from displacement data. *Journal of Geophysical Research* 112, B03207. <http://dx.doi.org/10.1029/2006JB004379>.
- Peltier, A., Famin, V., Bachèlery, P., Cayol, V., Fukushima, Y., Staudacher, T., 2008. Cyclic magma storages and transfers at Piton de la Fournaise volcano (La Réunion hotspot) inferred from deformation and geochemical data. *Earth and Planetary Science Letters* 270, 180–188.
- Peltier, A., Bachèlery, P., Staudacher, T., 2009a. Magma transport and storage at Piton de la Fournaise (La Réunion) between 1972 and 2007: a review of geophysical and geochemical data. *Journal of Volcanology and Geothermal Research* 184, 93–108.
- Peltier, A., Staudacher, T., Bachèlery, P., Cayol, V., 2009b. Formation of the April 2007 caldera collapse at Piton de la Fournaise volcano: insight from GPS data. *Journal of Volcanology and Geothermal Research* 184, 152–163.
- Poland, M.P., Sutton, A.J., Gerlach, T.M., 2009. Magma degassing triggered by static decompression at Kilauea Volcano, Hawaii. *Geophysical Research Letters* 36, L16306. <http://dx.doi.org/10.1029/2009GL039214>.
- Richter, F.M., Davis, A.M., DePaolo, D.J., Watson, E.B., 2003. Isotope fractionation by chemical diffusion between molten basalt and rhyolite. *Geochimica et Cosmochimica Acta* 67, 3905–3923.
- Rowe, M.C., Kent, A.J.R., Thornber, C.R., 2008. Using amphibole phenocrysts to track vapor transfer during magma crystallization and transport: an example from Mount St. Helens, Washington. *Journal of Volcanology and Geothermal Research* 178, 593–607.
- Rubin, K., 1997. Degassing of metals and metalloids from erupting seamount and mid-ocean ridge volcanoes: observations and predictions. *Geochimica et Cosmochimica Acta* 61, 3525–3542.
- Salaün, A., Villemant, B., Semet, M.P., Staudacher, T., 2010. Cannibalism of olivine-rich cumulate xenoliths during the 1998 eruption of Piton de la Fournaise (La Réunion hotspot): implications for the generation of magma diversity. *Journal of Volcanology and Geothermal Research* 198, 187–204.
- Schiano, P., David, K., Vlastélic, I., Gannoun, A., Klein, M., Nauret, F., Bonnard, P., 2012. Osmium isotope systematics of historical lavas from Piton de la Fournaise (Réunion Island, Indian Ocean). *Contributions to Mineralogy and Petrology*. <http://dx.doi.org/10.1007/s00410-012-0774-0>.
- Staudacher, T., Aki, K., Bachèlery, P., Catherine, P., Ferrazzini, V., Hochard, D., Kowalski, P., Ricard, L.P., Villeneuve, N., Cheminée, J.L., 2001. Piton de la Fournaise volcano, Réunion island, starts a new cycle of high eruptive activity. *Journal of Conference Abstracts* 6, 825.
- Staudacher, T., Ferrazzini, V., Peltier, A., Kowalski, P., Boissier, P., Catherine, P., Lauret, F., Massin, F., 2009. The April 2007 eruption and the Dolomieu crater collapse, two major events at Piton de la Fournaise (La Réunion Island, Indian Ocean). *Journal of Volcanology and Geothermal Research* 184, 126–137.
- Stieltjes, L., Moutou, P., 1989. A statistical and probabilistic study of the historic activity of Piton de la Fournaise, Réunion Island, Indian Ocean. *Journal of Volcanology and Geothermal Research* 36, 67–86.

- Sun, W., Arculus, R.J., Kamenetsky, V.S., Binns, R.A., 2004. Release of gold-bearing fluids in convergent margin magmas prompted by magnetite crystallization. *Nature* 431, 975–978.
- Tessalina, S.G., Yudovskaya, M.A., Chaplygin, I.V., Birck, J.-L., Capmas, F., 2008. Sources of unique rhenium enrichment in fumaroles and sulphides at Kudryavy volcano. *Geochimica et Cosmochimica Acta* 72, 889–909.
- Toramaru, A., 2006. BND (bubble number density) decompression rate meter for explosive volcanic eruptions. *Journal of Volcanology and Geothermal Research* 154, 303–316.
- Tulet, P., Villeneuve, N., 2011. Large scale modeling of the transport, chemical transformation and mass budget of the sulfur emitted during the April 2007 eruption of Piton de la Fournaise. *Atmospheric Chemistry and Physics* 11, 4533–4546.
- Vernet, M., Marin, L., Boulmier, S., Lhomme, J., Demange, J.C., 1987. Dosage du Fluor et du Chlore dans les matériaux géologiques y compris les échantillons hyperalumineux. *Analysis* 15, 490–498.
- Villemant, B., Salaün, A., Staudacher, T., 2009. Evidence for a homogeneous primary magma at Piton de la Fournaise (La Réunion): a geochemical study of matrix glass, melt inclusions and Pélé's hairs of the 1998–2008 eruptive activity. *Journal of Volcanology and Geothermal Research* 184, 79–92.
- Vlastélic, I., Staudacher, T., Semet, M., 2005. Rapid change of lava composition from 1998 to 2002 at Piton de la Fournaise (Réunion) inferred from Pb isotopes and trace elements: evidence for variable crustal contamination. *Journal of Petrology* 46, 79–107.
- Vlastélic, I., Peltier, A., Staudacher, T., 2007. Short-term (1998–2006) fluctuations of Pb isotopes at Piton de la Fournaise volcano (Réunion Island): origins and constraints on the size and shape of the magma reservoir. *Chemical Geology* 244, 202–220.
- Vlastélic, I., Deniel, C., Bosq, C., Télouk, P., Boivin, P., Bachèlery, P., Famin, V., Staudacher, T., 2009. Pb isotope geochemistry of Piton de la Fournaise historical lavas. *Journal of Volcanology and Geothermal Research* 184, 63–78.
- Vlastélic, I., Staudacher, T., Bachèlery, P., Télouk, P., Neuville, D., Benbakkar, M., 2011. Lithium isotope fractionation during magma degassing: constraints from silicic differentiates and natural gas condensates from Piton de la Fournaise volcano (Réunion Island). *Chemical Geology* 284, 26–34.
- Welsch, B., Faure, F., Bachèlery, P., Famin, V., 2009. Microcrysts record transient convection at Piton de la Fournaise volcano (La Réunion Hotspot). *Journal of Petrology* 50, 2287–2305.